Screening anlotinib responders via blood-based proteomics in non-small cell lung cancer

Jun Lu

   Shanghai Jiao Tong University Affiliated Chest Hospital

Wei Zhang

   Shanghai Jiao Tong University Affiliated Chest Hospital

Keke Yu

   Shanghai Jiao Tong University Affiliated Chest Hospital

Lele Zhang

   Shanghai Jiao Tong University Affiliated Chest Hospital

Yuqing Lou

   Shanghai Jiao Tong University Affiliated Chest Hospital

Ping Gu

   Shanghai Jiao Tong University Affiliated Chest Hospital

Wei Nei

   Shanghai Jiao Tong University Affiliated Chest Hospital

Jie Qian

   Shanghai Jiao Tong University Affiliated Chest Hospital

Jun Xu

   Anhui Medical University

Huimin Wang

   Shanghai Jiao Tong University Affiliated Chest Hospital

Hua Zhong

   Shanghai Jiao Tong University Affiliated Chest Hospital

Baohui Han (✉ 18930858216@163.com)

   Shanghai Jiao Tong University Affiliated Chest Hospital   https://orcid.org/0000-0002-3950-3030

Research

Abstract

Anlotinib has been demonstrated to be effective in advanced non-small cell lung cancer (NSCLC) patients. The response stratification of anlotinib remains unclear. In this study, plasma samples from 28 anlotinib-treated NSCLC patients (discovery cohort: 14 responders and 14 non-responders) were subjected to proteomic analysis, and plasma samples from 35 anlotinib-treated NSCLC patients (validation cohort) were subjected to validation analysis. Liquid chromatography-tandem mass spectrometry analysis was performed on samples with different time points, namely baseline (BL), best response (BR), and progression disease (PD). Bioinformatics analysis was performed to screen for the underlying differential proteins. Enzyme-linked immunosorbent assay was performed to detect plasma ARHGDIB, FN1, CDH1, and KNG1 levels respectively. The Kaplan-Meier survival analysis was used for biomarker-based responsive stratification. Our results indicated that differential proteins between responders and non-responders showed that proteomic technology potentially contributes to biomarker screening in plasma samples at BL. Furthermore, our results suggested that the detection of plasma ARHGDIB, FN1, CDH1, and KNG1 levels have potential predictive value for anlotinib response both in discovery cohort and validation cohort. Collectively, this study offers novel insights into the value of plasma biomarker screening via proteomic examination and suggests that plasma ARHGDIB, FN1, CDH1, and KNG1 levels could be used as biomarkers for anlotinib stratification in NSCLC patients.

1. Background

Anlotinib has been used for third-line or after third-line therapy in advanced non-small cell lung cancer (NSCLC) patients in China (1, 2). Clinical evidence has demonstrated that anlotinib significantly prolongs the progression-free survival (PFS) (anlotinib vs. placebo; 5.37 vs. 1.40 months) and median overall survival (OS) (anlotinib vs. placebo; 9.63 vs. 6.30 months) at third-line or after third-line therapy (1). Recent studies have indicated that anlotinib brings survival benefits to NSCLC patients and enhances the survival time of other types of cancers, such as small cell lung cancer (SCLC) and renal cell carcinoma (RCC) (3-5). Mechanistically, anlotinib-induced inhibition of angiogenesis and proliferative signaling contributes to the clinical phenomenon (6, 7). Further evidence indicates the targets of anlotinib, such as the chemokine ligand 2 (CCL2), receptor tyrosine kinases vascular endothelial growth (VEGFR), platelet derived growth factor receptor (PDGFR), and fibroblast growth factor receptor (FGFR) signaling pathways (8, 9). Therefore, the multi-target characteristics of this tyrosine kinase inhibitor (TKI) make clinical biomarker screening difficult.

In recent years, our study suggested that anlotinib-induced CCL2 decrease could potentially be used as a predictive factor for clinical stratification (8). Furthermore, blood KLK5 and L1CAM levels have also demonstrated potential value for the screening of anlotinib responders (10). Subsequently, next-generation sequencing (NGS) for plasma cell-free DNA (cfDNA) plays a role in anlotinib-responsive stratification, and the biomarker tumor mutation index (TMI) plus $IDH1^{exon4}$ mutation status can significantly identify anlotinib responders (11). In addition, other recent studies introduced predictors, including CD31-labeled circulating endothelial cells and baseline characteristics of patients, for the

stratification of patients treated with anlotinib (12-14). Although multiple attempts have been made, the effective biomarker for anlotinib stratification remains unclear. Due to the complex architecture of the anlotinib-induced anti-angiogenic signaling pathway (15), the importance of investigating plasma samples through a proteomic approach to identify patients who will have a positive response to anlotinib has not yet been justified. Therefore, we performed proteomic analysis on the plasma samples (anlotinib responders and anlotinib non-responders) and sought to examine its predictive value for anlotinib stratification.

2. Methods

2.1. Selection of patients: In the ALTER0303 study (https: //clinicaltrials.gov/ NCT02388919), a total of 440 qualified advanced NSCLC patients were enrolled and completed the clinical study. Among the sample libraries, we selected 28 patients as the discovery cohort according to the following three criteria: 1. non-responders (PFS < 60 days) with the best clinical objective response were defined as progression disease (PD); responders (PFS > 80 days) with the best clinical objective response were defined as partial response (Supplementary Table 1). 2. The plasma samples were collected from the same patient at different time points (baseline (BL), best response (BR), and PD). 3. All plasma samples passed quality control (including blood collection, centrifugation, plasma collection, and so on). Briefly, the plasma samples from 14 anlotinib non-responders at two time points of BL and PD and the plasma samples from 14 anlotinib responders at three time points: BL, BR, and PD were considered for this study (Fig. 1). The clinical characteristics of the 28 NSCLC patients are shown in Supplementary Table 1 and 2. All other administration and clinical care information has been introduced in our previous study (1, 2). Furthermore, we picked out 35 patients who were without the limitations of specific clinical characteristics as the validation cohort and collected the plasma samples at BL for biomarker validation.

2.2. Plasma collection and processing: The samples were collected as per standard procedures. Briefly, peripheral blood samples from advanced NSCLC patients were collected using EDTA tubes. All samples were centrifuged (1,600 × g for 10 min) within 2 h of blood collection. Then, the upper plasma was transferred to 1 mL sterile Eppendorf tubes using a pipette and stored at -80 °C. Due to the limitation of plasma volume, mixed plasma was prepared for proteomic analysis in the present study. Seven plasma samples (patients No. 1-7) from responders at BL were mixed together. Each patient contributed 100 μL plasma, and a total of 700 μL plasma was mixed for protein extraction. Similar to the previous procedure, the other seven plasma samples (patients No. 8-14) from responders at BL were mixed as duplicates for protein extraction (Supplementary Table 1 and 3). Therefore, two mixed samples from responders at BL were used for proteomic analysis. This study evaluated three time points (BL, BR, and PD) for responders and two time points (BL and PD) for non-responders. The mixed samples for other time points were based on the procedures of samples from responders at BL. All samples were collected from the same batch of patients at different time points (Supplementary Table 3). Ethical approval for this study was obtained from the institutional ethics committee of the Shanghai Chest Hospital prior to commencing. Consent for all resources (including patients' clinical data, blood samples, and tumor samples) was obtained before clinical screening.

2.3. Protein extraction: Plasma samples of 700 μL were used for protein extraction. Each mixed sample was performed the removal of IgG, IgA, albumin, antitrypsin, haptoglobin, transferrin, and so on using a Thermo Scientific high-select top 14 abundant protein depletion resin kit (Thermo Fisher, USA) (Supplementary Table 4). As previous study introduced[16], each mixed sample was performed standard procedures including suspension (50 μL PBS); centrifugation (10,000 × g for 30 min in 4 °C); and then suspension using 100 μL lysis buffer (7 M urea, 2 M thiourea). The suspended samples were performed centrifugation at 40,000 × g for 30 min. Ultrasonic sonication were used for protein extraction. Protein samples were quantified using the bicinchoninic acid (BCA) method. Gel electrophoresis images of the total protein and the total protein without abundant protein were shown in Supplementary Fig. 1.

2.4. Protein digestion: Protein digestion was performed as previous described [16, 17]. Briefly, 300 μg of the total protein without abundant protein for each sample were subjected to enzymatic hydrolysis. DTT was added to a concentration of 100 mM, incubated at 100 °C for 5 min, and then cooled to room temperature. After precipitating with trichloroacetic acid for 30 min on ice, then diluted with 50 mM NH_4HCO_3 buffer to a final concentration of 0.5 mg/ml. The samples were performed digestion with trypsin at 37 °C for 12 h. Trifluoroacetic acid (TFA) was added to achieve 0.1% TFA in the solution, and desalination was performed using a C18 cartridge.

2.5. Liquid chromatography-tandem mass spectrometry (LC-MS/MS) analysis: Peptide mixtures were subjected to nano-liquid chromatography associated with MS for protein identification. MS analysis was performed on the abovementioned 15 components serially. High-performance liquid chromatography (HPLC, Agilent, USA) was used to separate the components. After separation, Q-Extractive Plus MS (Thermo Scientific, USA) was used for MS/MS analysis. Collection of desalting and separating samples were performed using a RP trap column (Thermo EASY column SC200, 150 μm × 100 mm) and a C18 reverse-phase column (Thermo EASY column SC100 traps, 150 μm × 20 mm). Mobile phase A consisted of HPLC-grade water containing 0.1% formic acid (FA), and phase B consisted of 84% HPLC-grade acetonitrile (ACN) containing 0.1% FA. The analytical separation was run at a flow rate of 400 nl/min by using a linear gradient of phase B as follows: 0–45% for 100 min, 45–100% for 8 min, and 100% for 12 min. Each LC-MS/MS analysis was repeated three times to reduce technical variation [18].

2.6 Data availability: Raw data were uploaded to MaxQuant software (version 1.6.0.16), and database retrieval was done (Supplementary Table 5). The database (Uniprot_Human_162254_20180320) website is https://www.uniprot.org/uniprot/?query=organism:9606. All raw data were deposited in the ProteomeXchange Consortium (http://proteomecentral.proteomexchange.org) via the iProX partner repository with the project ID: IPX017919.

2.7. Differentially proteins analysis: This study performed differential proteins comparison among different groups (responders and non-responders) and different time points (BL, BR, and PD). For the anlotinib responders, we compared the differential proteins between the two time points of BL and BR; and compared the differential proteins between the three time points of BL, BR and PD. For the anlotinib non-responders, we compared the differential proteins between the two time points of BL and PD.

Furthermore, we compared the differential proteins between responders and non-responders, at different time points of BL and PD respectively.

2.8. Bioinformatics analysis: Protein clustering was performed on the differentially proteins between different samples. Similar to our previous study ([19](), [20]()), Gene Ontology (GO) analysis and Kyoto Encyclopedia of Genes and Genomes (KEGG) pathway analysis were performed using a public bioinformatics resource platform (DAVID, https://david.ncifcrf.gov/) by uploading the differential gene lists. Under GO analysis, biological processes, molecular functions, and cellular components were used to characterize the differential proteins.

2.9. Integrative analysis for upregulated proteins and downregulated proteins: We performed the integrative analysis to compare the protein levels of responders and the protein levels of non-responders at BL. These proteins with significantly higher or lower levels in responder at BL were screened out for further analysis. Next, we compared these high or low levels of proteins to the all proteins of responders at BR, and screened out the upregulated proteins and downregulated proteins respectively. Lastly, we compared the above screened proteins to the all proteins of responders at PD, and screened out the upregulated proteins and downregulated proteins of responders at BL respectively.

2.10. Detection of plasma protein levels and anlotinib responsive analysis: The enzyme-linked immunosorbent assay (ELISA) kit for ARHGDIB detection was purchased from Cloud-Clone Corporation (CHN). The ELISA kits for FN1, CDH1, and KNG1 were purchased from Abcam (UK). The experimental procedures were performed according to the manufacturer's instructions. Here, we allocated the 28 NSCLC patients (including 14 responders and 14 non-responders) who received anlotinib as discovery cohort, and allocated the 35 NSCLC patients who received anlotinib as validation cohort. Plasma samples from discovery cohort and validation cohort were detected at the time point of BL. Based on the levels of ARHGDIB, FN1, CDH1, and KNG1, the binary bit method was used for responsive stratification in discovery cohort as previously reported ([21-24]()). The cutoff values were used for testing the stratification effects in the validation cohort.

2.11. Statistical analysis: Due to the biological repetition was set as two in the present study, the t-test *P* value can not be calculated. Therefore, the significance of differentially proteins was calculated according to foldchange, without processed statistical adjustment. PFS and OS were summarized as median values and two-sided 95% confidence intervals and were analyzed using the Kaplan-Meier method. The Mantel-Cox test was used to perform the Kaplan-Meier survival analysis using GraphPad Prism 5. Differences were considered significant at $P < 0.05$, $P < 0.01$, and $P < 0.001$.

3. Results

3.1. Comparison of the differential proteins between baseline and best response in anlotinib responders

In this study, 14 patients without any anlotinib response (median PFS: 35.5 days; median OS: 158.5 days), and 14 patients with superior anlotinib response (median PFS: 189 days; median OS: 373 days)

were subjected to proteomic analysis (Fig. 1, Supplementary Table 2). There is no significant difference between responders and non-responders based on the clinical characteristics such as age, gender, smoking history, etc. (Supplementary Table 2). Here, we first examined the differential proteins in the anlotinib responders at the time point of BL. After anlotinib administration, 470 different proteins were detected via quantitative proteomics. Of the 470 proteins, 28 protein levels at BL (FABP5, KRT6C, CALML5, KRT17, HIST1H4H, TXN, KRT16, WDR11, KRT1, CCDC87, PRSS1, GAPSH, LTF, S100A8, A8K5J8 (Protein ID), KRT5, SPDL1, HSP90AB1, DKFZp667J0810, S100A9, KRT10, MASP1, F5, SLC38A3, Q9UL82 (Protein ID), HYDIN, PROC, DKFZp686O16217) were lower and 30 protein levels at BL (SERPINA1, CASP14, OGN, SAA1, A0A125U0U7 (Protein ID), TTLL5, PSME4, APOB, CRP, ALDOC, RAB1, HBA2, HRNR, SAA1, SSFA2, CEP110, MRC1L1, STAB1, CALM2, THBS1, HLA-A, CD99, ORF1 5, TMSB4X, TRIM33, MMRN1, LRP1, CST3, ARHGDIB, IGHD) were higher than those of BR (Fig. 2a). Subsequently, we performed biological process and cell component analysis of the 58 differentially proteins. The results suggested that these proteins are involved in single-multicellular organism and multicellular organismal processes after biological process analysis, and these proteins are also involved in the extracellular region after cell component analysis (Fig. 2b). Furthermore, biological process analysis suggested that the up-regulated proteins were enriched in the single-multicellular organism process, multicellular organismal process and biological regulation, and the down-regulated proteins were enriched in the protein metabolic, organonitrogen compound metabolic, and nitrogen compound metabolic processes (Fig. 2c). These results suggested that anlotinib-induced plasma protein level alterations may affect the different biological processes, cell components, and signaling pathways, which are potentially involved in anti-tumor effect.

3.2. Proteomic analysis in anlotinib responders from baseline to progression disease

To analyze the dynamic changes of the differential proteins from BL to PD, we further compared the plasma protein levels of responders at three time points: BL, BR, and PD. A total of 18 proteins were screened and showed significant alterations. Heat map analysis indicated that level of 7 proteins (F7, PROC, LCAT, ATRN, IGFBP3, GGH, DKFZp686M0562) increased at the time point of BR, then decreased at the time point of PD. The level of 7 proteins (ALDOA, LMAN2, PFN1, MUC5B, Q53GW0 (Protein ID), FGG, SH3BGRL3) increased continually and the level of 1 protein (CD163) decreased continually after anlotinib administration. The level of 3 proteins (FGA, GOLPH2, TREML1) decreased at the time point of the BR and then increased at the time point of PD (Fig. 3a). Biological process analysis suggested that these 18 proteins were enriched in processes such as platelet activation, cell activation, and blood coagulation. Cell component analysis suggested that these proteins were enriched in cell membrane-bound vesicles, extracellular space, and vesicles (Fig. 3b). KEGG pathway analysis indicated that these proteins were enriched in signaling pathways including shigellosis, complement and coagulation cascades, *Salmonella* infection, and salivary secretion (Fig. 3c). These results suggested that anlotinib-induced plasma protein level alterations at different time points may affect the different biological processes, cell components, and signaling pathways, which are potentially involved in acquired resistance.

3.3. Analysis of primary resistance to anlotinib via proteomic characterization

To screen the primary resistant plasma protein markers of anlotinib via proteomic characterization, we first compared the differential proteins after anlotinib administration among non-responders at two time points, BL and PD. Compare to BL of non-responders, a total of 41 differentially proteins were screened via proteomic analysis in plasma samples from PD of non-responders. Of these 41 proteins, it was found that the level of 20 proteins (COL19A1, TF, B4E1B2 (Protein ID), NXPE1, VH6DJ, PDXDC1, PRSS1, A8K5J8 (Protein ID), A2J1N6 (Protein ID), IGKV4-1, APOB, KRT16, DKFZp686K03196, SPDL1, FGB, Q9UL82 (Protein ID), KNG1, FGG, FLJ00385, AOAOX9v9B3 (Protein ID)) was significantly increased and the level of 21 proteins (CALML5, ARGHDIB, CALM2, CDH1, SAA1, ALDOC, Q53GW0 (Protein ID), FN1, Q9UE53 (Protein ID), OGN, PAPOLA, APOB, TMSB4X, HEL-S-108, STAB1, ZBTB18, A0A0S2Z3V0 (Protein ID), KRT2, ITIH1, S100A12, VCL) was remarkably decreased (Fig. 4a). Biological process analysis suggested that these proteins were enriched in processes such as cell migration, cell localization, and cell motility (Fig. 4b). Further analysis indicated that the up-regulated proteins were enriched in metabolic, organic substance metabolic, and cellular processes. The down-regulated proteins were enriched in endocytosis, receptor-mediated endocytosis, and chemical homeostasis (Fig. 4c). Cell component analysis suggested that these proteins were enriched in extracellular regions and vesicles (Fig. 4b). These results suggested that these proteins may play important roles in tumor cell-activating compensatory effects to relieve anlotinib stress.

Furthermore, the differential proteins between responders and non-responders at BL are still unclear. Here, we identified 470 proteins that existed in the BL samples from responders and non-responders. Compared to the non-responders, 23 proteins (CASP14, CFI, COL19A1, HLA-A, IGHD, A125QYY9, SAA1, KNG1, LPA, THBS1, SOD3, B7Z539 (Protein ID), MRC1L1, CD99, DKFZp686K18196, RAB1, IGFBP6, CST3, COL6A1, ADIPOQ, C4B, EBM42, PZP, APOA2, C1R) were upregulated and 21 proteins (APOB, CDH1, AFTPH, APOE, KRT1, KRT2, ITIH1, ARHGDIB, CLEC3B, FN1, TXN, LTF, KRT10, CD4, HSP90AB1, SERPINA1, MENT, HEL-S-108, B7Z8Q7 (Protein ID), PAPOLA, S100A9) were downregulated in responders at BL (Fig. 5a, 5b). These differential proteins are enriched in biological processes like peptide cross-linking, regulation of peptidase activity, and cornification (Fig. 5c). Cell component analysis suggested that these differentially proteins were enriched in the extracellular space and region (Fig. 5c). In particular, these up-regulated proteins in responders were enriched in responses to stimuli, biological regulation, and regulation of biological processes, while the down-regulated proteins were enriched in the cellular macromolecule metabolic, nitrogen compound metabolic, and macromolecule metabolic processes (Fig. 5d). Furthermore, the differential proteins between responders and non-responders at the time of PD suggested that there were 15 proteins with higher levels in non-responders than those in non-responders, and 4 proteins with lower levels in non-responders than those of responders (Supplementary Fig. 2).

3.4. Integrative analysis reveals blood-based proteomics potentially be used for screening of anlotinib responders

To further screen out the potential plasma biomarker, integrative analysis was performed on those differential proteins at three time points: BL, BR, and PD from responders and at the time point of BL from non-responders. After the filtered analysis, we found that 43 differentially proteins (38 proteins with low level and 5 proteins with high level) of responders at BL showed important potential values (Fig. 6a). For the samples from non-responders at BL, of 43 proteins, 5 proteins (COL19A1, KNG1, CF1, RBM42, APOA2) were found to have lower levels, and 38 proteins (ARHGDIB, FN1, CDH1, MENT, AFTPH, IGLC7, APOE, CLEC3B, KRT2, PAPOLA, CD4, CTDP1, HYOU1, PDIA3, IGHV3-30, CAMP, SERPINA1, FTL, TPM4, ACTB, SH3BGRL3, YWHAZ, MUC5B, CAPN1, ALDOA, LCN2, LAMA2, DAG1, PFN1, LTA4H, TAGLN2, LMAN2, FLNA, ENPP3, S100A6, S100A12, PPIA, SAA1) were found to have higher levels than those of responders at BL (Fig. 6a, 6b). Biological process analysis suggested that these proteins are enriched in receptor-mediated endocytosis, platelet degranulation, and innate immune response. Cellular component analysis suggested that these proteins are enriched in protein binding, poly (A) RNA binding, and calcium ion binding. Molecular function analysis suggested that these proteins are enriched in extracellular exosome, extracellular region and space (Fig. 6c). Based on these differential proteins, we detected the plasma ARHGDIB, FN1, CDH1, and KNG1 levels at BL in responders and non-responders, and found that low level of plasma ARHGDIB, FN1, and CDH1 in NSCLC patients had a better response to anlotinib than those patients with high level of plasma ARHGDIB, FN1, and CDH1 (Fig. 7a, Supplementary Fig. 3a). On the contrary, the NSCLC patients with high level of plasma KNG1 had a better response to anlotinib than those patients with low level of plasma KNG1 (Fig. 7a, Supplementary Fig. 3a). For understand whether this phenomenon can be validated in a validation cohort, we further detected the above proteins at BL in a 35 patients' cohort who also received anlotinib therapy (Supplementary Fig. 3b). Interestingly, the Kaplan-Meier plots analysis suggested that these plasma levels of proteins can also stratify the responders and non-responders in validation cohort (Fig. 7b). Collectively, these results suggested that proteomics analysis can potentially be used for anlotinib-responsive stratification (Fig. 8).

4. Discussions

Anlotinib, a multi-target TKI inhibitor, has been demonstrated to be effective against different cancers in clinical trials (1, 3-5, 7). Due to the main mechanism of anti-angiogenesis, the complex architecture of the signaling pathway limits anlotinib biomarker screening (11). Previous studies have discussed potential anlotinib biomarkers (8, 10, 11, 20). However, the effective biomarker for anlotinib stratification remains unclear. In order to screen for potential biomarkers, we performed proteomics on plasma samples from anlotinib responders and anlotinib non-responders.

Proteomic technology has been widely used in biomedical research since its establishment (25-28). For example, Jiang et al. found that proteomics could identify novel therapeutic targets for hepatocellular carcinoma (29); Eckert et al. suggested that the metabolic regulator *NNMT* can be screened out via proteomics (30). Along with technology development, cancer biomarker screening based on proteomics has been introduced in clinical translational research (27, 31, 32). Whether proteomic technology can be used for biomarker screening of the anlotinib-induced complex anti-angiogenic signaling pathway is still unclear. Furthermore, the development of liquid biopsy is changing the clinical practice of cancer (27, 33-

35). Studies have shown the potential value of screening cancer biomarkers from blood via proteomics (27, 36-39). However, proteomics-based liquid biopsy-guided cancer treatment still requires further exploration (27).

In the present study, we first compared the changes in plasma protein levels in anlotinib responders between BL and BR and found that proteins with significantly increased or decreased levels may play an important role in anlotinib-induced antitumor effects. After comparing the plasma protein levels at three different time points (BL, BR, and PD) in anlotinib responders, we found that eight differentially proteins were potentially associated with anlotinib-acquired resistance. Lastly, after integrating analysis of responders and non-responders at different time points (BL, BR, and PD), the results suggested that 43 differential proteins could potentially be used as biomarkers. Of the 43 differential proteins, ARHGDIB, FN1, CDH1, and KNG1 were demonstrated to be potentially effective for screening anlotinib responders in the present study. However, whether these plasma proteins were derived from cancer cells or normal tissue cells need to be further discussed. Interestingly, we found the binding proteins including FN1 and CDH1 in the present study as well as the binding protein L1CAM in our previous report (10) potentially played an important role for predicting anlotinib response. Although we found many differential proteins between anlotinib responders and anlotinib non-responders, the methods for sample preparation (such as mixed samples) still need to be optimized. Furthermore, significant difference of serval proteins observed between duplicated samples also should be concerned. Whether individual variation or technology bias need to further discussion. The main limitation of the present study was using a mixture of the seven samples as one testing sample. In the future, proteomic analysis should be performed on individual samples for further validation. Nevertheless, the present study provides an interesting approach for anlotinib biomarker screening via proteomic technology.

5. Conclusion

In conclusion, our study provides a new perspective of plasma biomarker screening via proteomic examination, and suggests that blood-based proteomics could potentially be used as a biomarker for anlotinib stratification in NSCLC patients.

Declarations

Acknowledgements

Author contributions

Experiments were conceived and designed by B.H. Han, H. ZHong and J. Lu. Clinical analysis, bioinformatics analysis and statistical analysis were performed by J. Lu, W. Zhang, K.K. Yu, Y.Q. Lou, J. Xu, L.L. Zhang, P. Gu, W. Nie, and J. Qian. Figures and tables were generated by J. Lu, H. Zhong, W. Zhang, K.K. Yu, and H.M. Wang, and the manuscript was written by J. Lu. The manuscript was revised by B.H. Han and H. Zhong.

Competing financial interest statement

The authors declare no competing financial interest.

References

1.   Han, B. H., Li, K., Wang, Q. M., *et al.* Effect of Anlotinib as a Third-Line or Further Treatment on Overall Survival of Patients With Advanced Non-Small Cell Lung Cancer The ALTER 0303 Phase 3 Randomized Clinical Trial. *JAMA oncology.* 2018; **4**: 1569-1575.

2.   Han, B. H., Li, K., Zhao, Y. Z., *et al.* Anlotinib as a third-line therapy in patients with refractory advanced non-small-cell lung cancer: a multicentre, randomised phase II trial (ALTER0302). *BrJ Cancer.* 2018; **118**: 654-661.

3.   Cheng, Y., Wang, Q., Li, K., *et al.* Overall survival (OS) update in ALTER 1202: Anlotinib as third-line or further-line treatment in relapsed small-cell lung cancer (SCLC). *Ann Oncol.* 2019; **30**: v711.

4.   Chi, Y. H. B. L., Fang, Z. W., Hong, X. N., *et al.* Safety and Efficacy of Anlotinib, a Multikinase Angiogenesis Inhibitor, in Patients with Refractory Metastatic Soft-Tissue Sarcoma. *Clin Cancer Res.* 2018; **24**: 5233-5238.

5.   Zhou, A.-P., Ma, J., Bai, Y., *et al.* Anlotinib versus sunitinib as first line treatment for metastatic renal cell carcinoma (mRCC): Preliminary results from a randomized phase II clinical trial. *J Clin Oncol.* 2016: 4565-4565.

6.   Xie, C. Y., Wan, X. Z., Quan, H. T., *et al.* Preclinical characterization of anlotinib, a highly potent and selective vascular endothelial growth factor receptor-2 inhibitor. *Cancer Sci.* 2018; **109**: 1207-1219.

7.   Sun, Y., Niu, W., Du, F., *et al.* Safety, pharmacokinetics, and antitumor properties of anlotinib, an oral multi-target tyrosine kinase inhibitor, in patients with advanced refractory solid tumors. *J Hematol Oncol.* 2016; **9**: 105.

8.   Lu, J., Zhong, H., Chu, T., *et al.* Role of anlotinib-induced CCL2 decrease in anti-angiogenesis and response prediction for nonsmall cell lung cancer therapy. *Eur Respir J.* 2019; **53**: 1801562.

9.   Lin, B. Y., Song, X. M., Yang, D. W., Bai, D. S., Yao, Y. Y., and Lu, N. Anlotinib inhibits angiogenesis &ITvia&IT suppressing the activation of VEGFR2, PDGFR beta and FGFR1. *Gene.* 2018; **654**: 77-86.

10.   Lu, J., Shi, Q., Zhang, L., *et al.* Integrated transcriptome analysis reveals KLK5 and L1CAM predict response to anlotinib in NSCLC at 3rd line. *Front Oncol.* 2019; **9**: 886.

11.   Lu, J., Zhong, H., Wu, J., *et al.* Circulating DNA-Based Sequencing Guided Anlotinib Therapy in Non-Small Cell Lung Cancer. *Adv Sci.* 2019; **6**: 1900721.

12.   Liu, Z. J., Wang, J., Meng, Z. T., *et al.* CD31-labeled circulating endothelial cells as predictor in anlotinib-treated non-small-cell lung cancer: Analysis on ALTER-0303 study. *Cancer Med.* 2018; **7**: 3011-3021.

13.   Wang, J., Zhao, Y., Wang, Q., *et al.* Prognostic factors of refractory NSCLC patients receiving anlotinib hydrochloride as the third-or further-line treatment. *Cancer Biol Med.* 2018; **15**: 443-451.

14.   Shen, Y., Lu, J., Hu, F., *et al.* Effect and outcomes analysis of anlotinib in non-small cell lung cancer patients with liver metastasis: results from the ALTER 0303 phase 3 randomized clinical trial. *J Cancer Res Clin Oncol.* 2022; doi: 10.1007/s00432-022-03964-9.

15.   Pilotto, S., Bonomi, M., Massari, F., *et al.* Anti-angiogenic drugs and biomarkers in non-small-cell lung cancer: a 'hard days night'. *Curr Pharm Des.* 2014; **20**: 3958-3972.

16.   Li, J., Sun, L., Xu, F., *et al.* Screening and Identification of APOC1 as a Novel Potential Biomarker for Differentiate of Mycoplasma pneumoniae in Children. *Front Microbiol.* 2016; **7**: 1961.

17.   Fujita, K., Kume, H., Matsuzaki, K., *et al.* Proteomic analysis of urinary extracellular vesicles from high Gleason score prostate cancer. *Sci Rep.* 2017; **7**: 42961.

18.   Lee, J., Kim, S. H., Choi, D. S., *et al.* Proteomic analysis of extracellular vesicles derived from Mycobacterium tuberculosis. *Proteomics.* 2015; **15**: 3331-3337.

19.   Lou, Y., Xu, J., Zhang, Y., *et al.* Akt kinase LANCL2 functions as a key driver in EGFR-mutant lung adenocarcinoma tumorigenesis. *Cell Death Dis.* 2021; **12**: 170.

20.   Lu, J., Xu, W., Qian, J., *et al.* Transcriptome profiling analysis reveals that CXCL2 is involved in anlotinib resistance in human lung cancer cells. *BMC Med Genomics.* 2019; **12**: 38.

21.   Chu, T., Lu, J., Bi, M., *et al.* Equivalent efficacy study of QL1101 and bevacizumab on untreated advanced non-squamous non-small cell lung cancer patients: a phase 3 randomized, double-blind clinical trial. *Cancer Biol Med.* 2021; **18**: 816-824.

22.   Zhang, Y., Sun, B., Hu, M., *et al.* CXCL9 as a Prognostic Inflammatory Marker in Early-Stage Lung Adenocarcinoma Patients. *Front Oncol.* 2020; **10**: 1049.

23.   Lu, J., Zhong, R., Lou, Y., *et al.* TP53 Mutation Status and Biopsy Lesion Type Determine the Immunotherapeutic Stratification in Non-Small-Cell Lung Cancer. *Front Immunol.* 2021; **12**: 732125.

24.   Lu, J., Chu, T., Liu, H., *et al.* Equivalent efficacy assessment of QL1101 and bevacizumab in nonsquamous non-small cell lung cancer patients: A two-year follow-up data update. *Chin J Cancer Res.* 2022; **34**, 28-39.

25.   Mann, M., and Jensen, O. N. Proteomic analysis of post-translational modifications. *Nature Biotechnol.* 2003; **21**: 255-261.

26.   Wulfkuhle, J. D., Liotta, L. A., and Petricoin, E. F. Proteomic applications for the early detection of cancer. *Nat Rev Cancer.* 2003; **3**: 267-275.

27.   Boccellino, M., Pinto, F., Ieluzzi, V., *et al.* Proteomics analysis of human serum of patients with non-small-cell lung cancer reveals proteins as diagnostic biomarker candidates. *J Cell Physiol.* 2019; **234**: 23798-23806.

28.   Peng, L., Cantor, D. I., Huang, C., Wang, K., Baker, M. S., and Nice, E. C. Tissue and plasma proteomics for early stage cancer detection. *Mol Omics.* 2018; **14**: 405-423.

29.   Jiang, Y., Sun, A., Zhao, Y., *et al.* Proteomics identifies new therapeutic targets of early-stage hepatocellular carcinoma. *Nature.* 2019; **567**: 257-261.

30.   Eckert, M. A., Coscia, F., Chryplewicz, A., *et al.* Proteomics reveals NNMT as a master metabolic regulator of cancer-associated fibroblasts. *Nature.* 2019; **569**: 723-728

31.   Hristova, V. A., and Chan, D. W. Cancer biomarker discovery and translation: proteomics and beyond. *Expert Rev Proteomics.* 2019; **16**: 93-103.

32.   Henderson, M. C., Silver, M., Tran, Q., *et al.* A noninvasive blood-based combinatorial proteomic biomarker assay to detect breast cancer in women over age 50 with BI-RADS 3, 4, or 5 Assessment. *Clin Cancer Res.* 2019; **25**: 142-149.

33.   Lu, J., and Han, B. H. Liquid Biopsy Promotes Non-Small Cell Lung Cancer Precision Therapy. *Technol Cancer Res Treatment.* 2018; **17**: 1533033818801809.

34.   Xu, W., Lu, J., Zhao, Q., *et al.* Genome-Wide Plasma Cell-Free DNA Methylation Profiling Identifies Potential Biomarkers for Lung Cancer. *Dis Markers.* 2019; **2019**: 4108474.

35.   Lu, J., Zhang, Y., Lou, Y., *et al.* ctDNA-Profiling-Based UBL Biological Process Mutation Status as a Predictor of Atezolizumab Response Among TP53-Negative NSCLC Patients. *Front Genet.* 2021; **12**: 723670.

36.   Kim, Y., Jeon, J., Mejia, S., *et al.* Targeted proteomics identifies liquid-biopsy signatures for extracapsular prostate cancer. *Nat Commun.* 2016; **7**: 1-10.

37.   Barnabas, G. D., Bahar-Shany, K., Sapoznik, S., *et al.* (2019) Microvesicle proteomic profiling of uterine liquid biopsy for ovarian cancer early detection. *Mol Cell Proteomics.* 2021; **18**: 865-875.

38.   Loriot, Y., Marabelle, A., Guegan, J. P., *et al.* Plasma proteomics identifies Leukemia Inhibitory Factor (LIF) as a novel predictive biomarker of immune-checkpoint blockade resistance. *Ann Oncol.* 2021; **32**: 1381-1390.

39.   Huang, Z., Ma, L., Huang, C., Li, Q., and Nice, E. C. Proteomic profiling of human plasma for cancer biomarker discovery. *Proteomics.* 2017: **17**: 1600240.

Figures
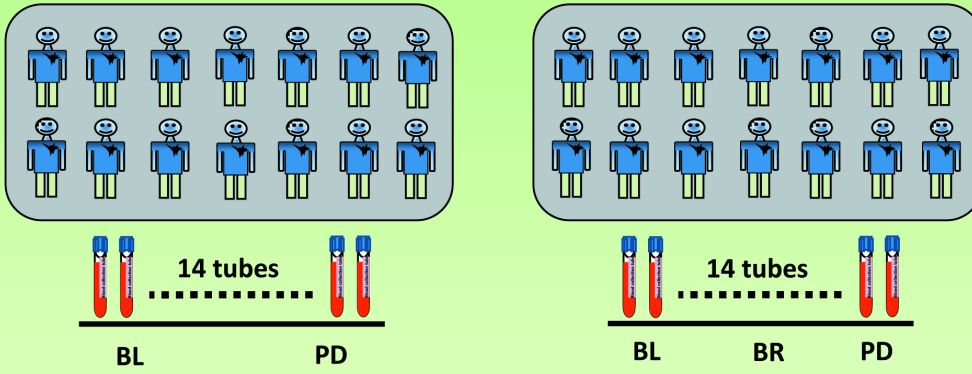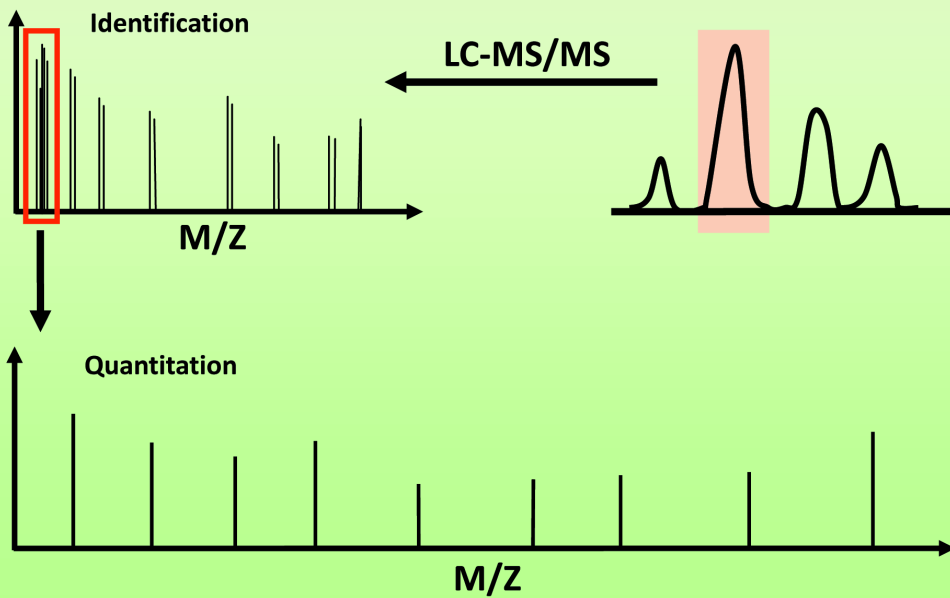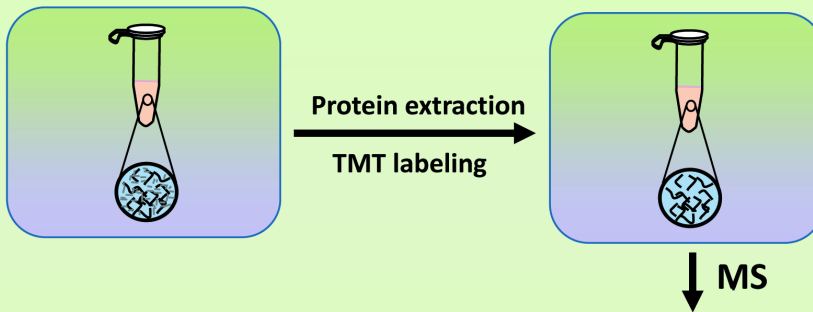
Figure 1

The flowchart of proteomics of plasma samples from NSCLC patients with anlotinib responders and anlotinib non-responders. Plasma samples were performed protein extraction, TMT labelling, LC-MS/MS identification, and quantitation for proteomics analysis. BL: the plasma was collected at baseline. BR: the plasma was collected at BR. PD: the plasma was collected at PD.
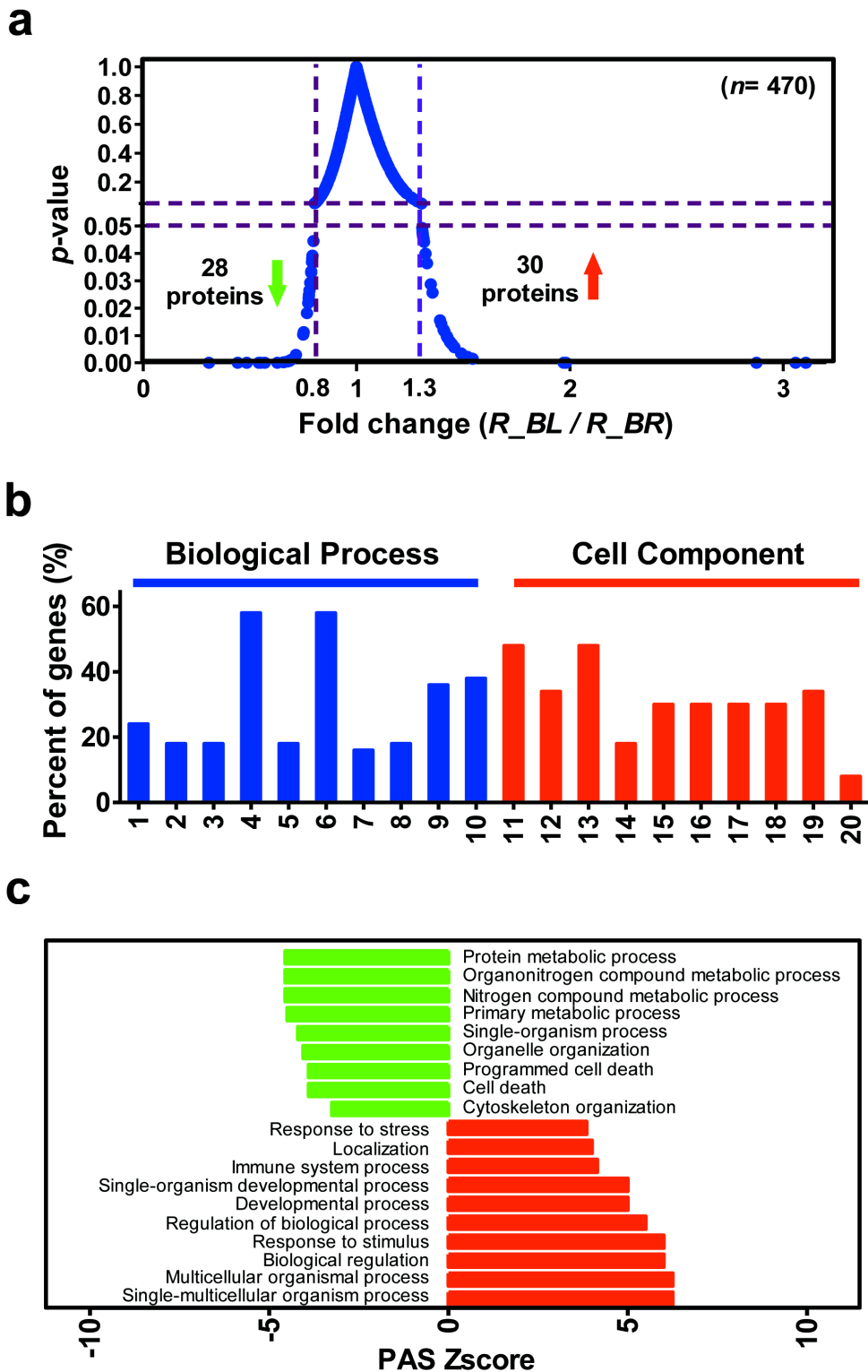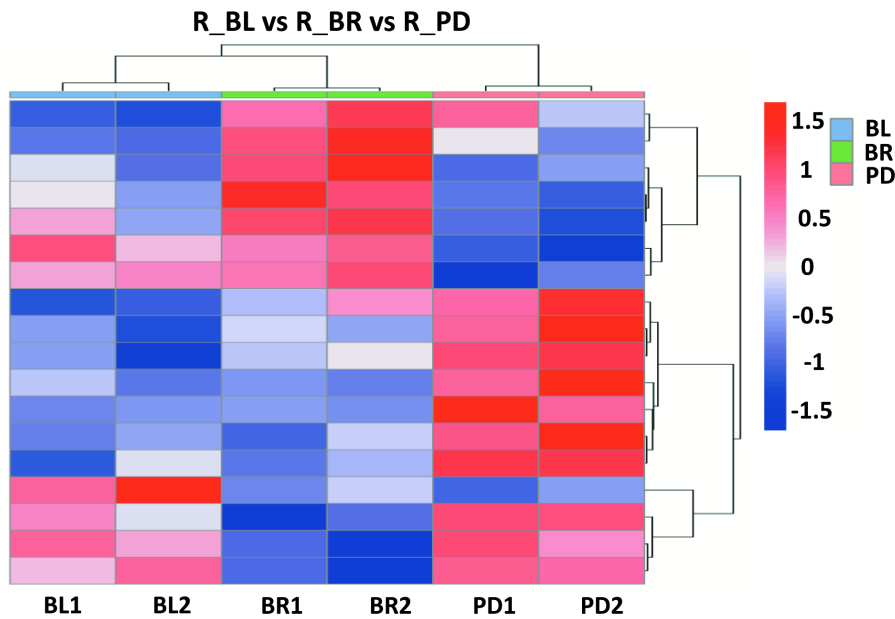
Figure 2

Analysis of the differential protein levels between baseline and best response in anlotinib responders. (a) Scatter plot analysis of the differential proteins (R_BL / R_BR)*. (b) Biological process and cell component analysis for those differential proteins#. (c) Biological process analysis for those up-regulated and down-regulated proteins respectively. *R_BL: the plasma collected from responders at BL. R_BR: the

plasma collected from responders at BR. #1. Inflammatory response; 2. Keratinization; 3. Acute inflammatory response; 4. Single-multicellular organism process; 5. Keratinocyte differentiation; 6. Multi-cellular organismal process; 7. Cornification; 8. Epidermal cell differentiation; 9. Immune response; 10. Immune system process; 11. Extracellular region part; 12. Extracellular space; 13. Extracellular region; 14. Intermediate filament cytoskeleton; 15. Extracellular membrane-bounded organelle; 16. Extracellular exosome; 17. Extracellular vesicle; 18. Extracellular organelle; 19. Membrane-bounded vesicle; 20. Cornified envelope.
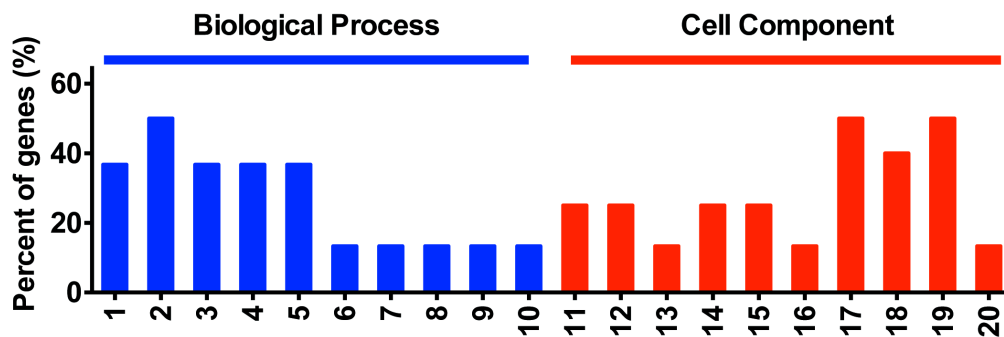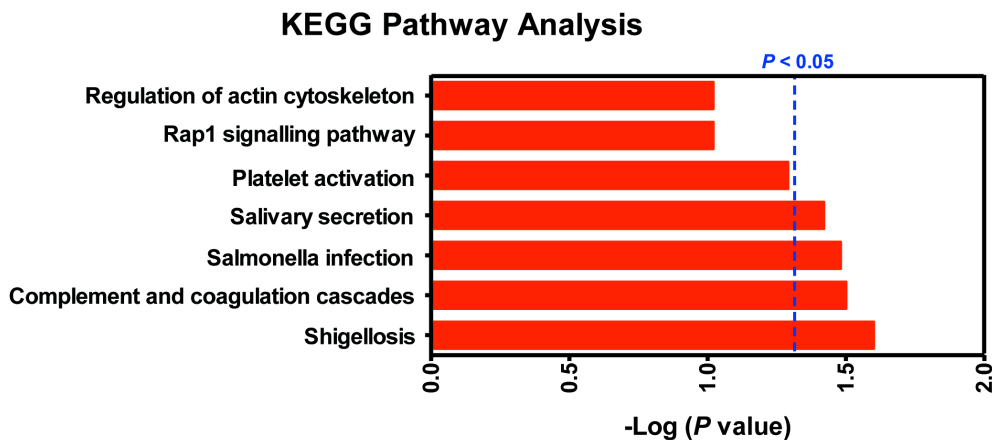
Figure 3
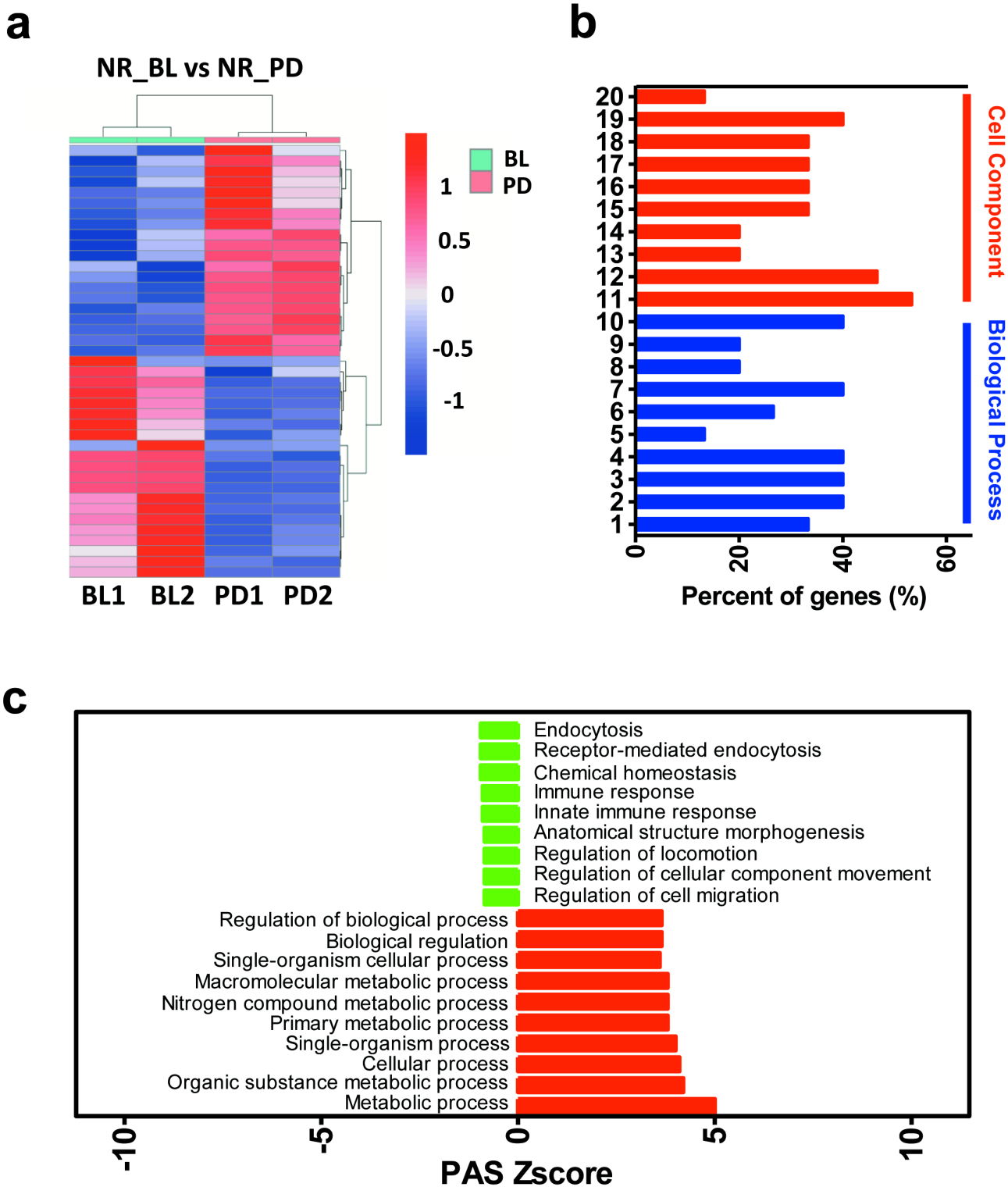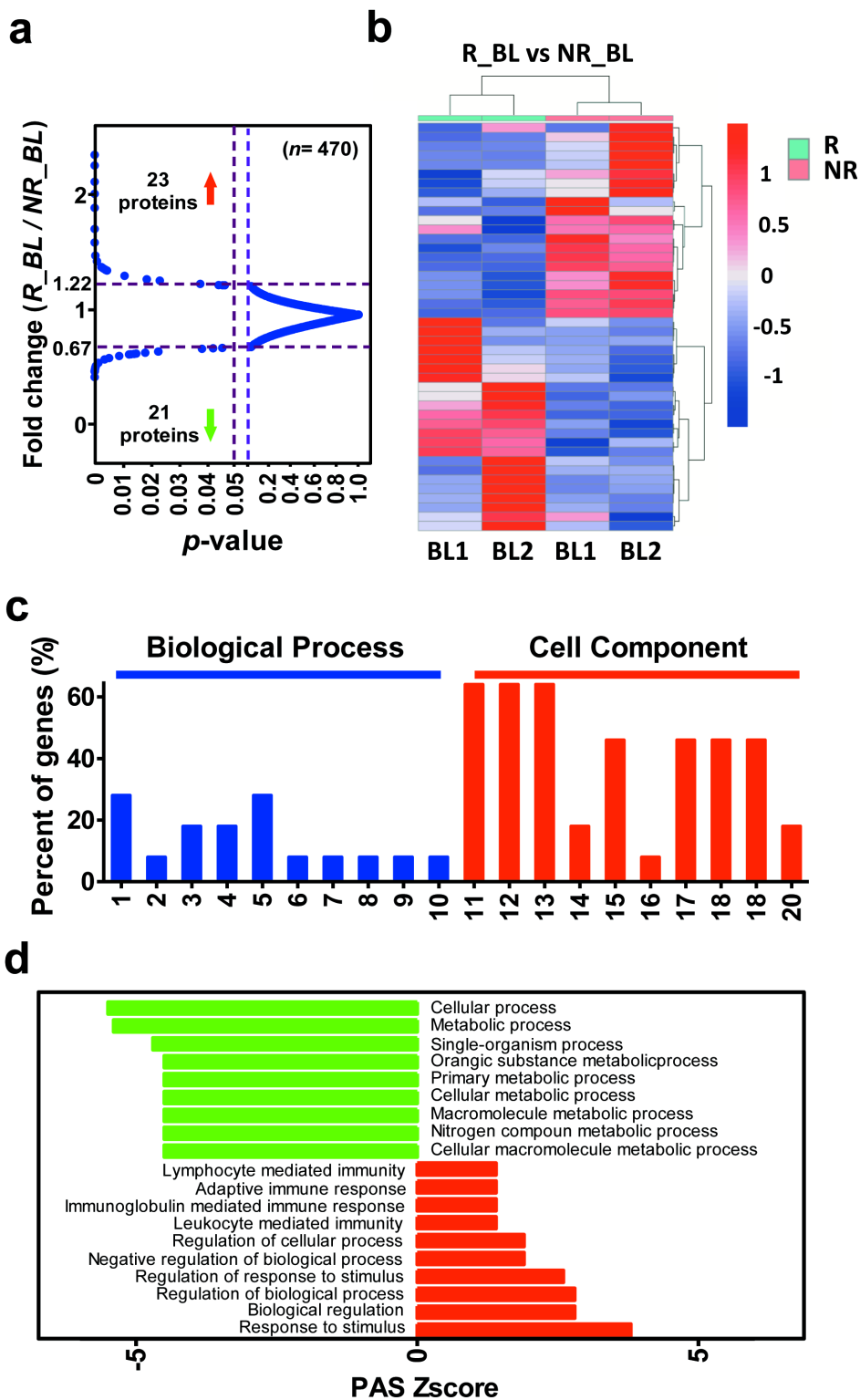
Integrative analysis of differential protein levels between baseline, best response, and progression disease in anlotinib responders. (a) Heat map representation of protein differentially levels between R_BL, R_BR and R_PD*. Each group contained 2 duplicate samples. The one sample represented the mean data of patients No. 1-7, and the other one represented the mean data of patients No. 8-14. (b) Biological process and cell component analysis for those differential proteins[#]. (c) KEGG pathways analysis of 18 differential proteins. *R_BL: the plasma collected from responders at BL. R_BR: the plasma collected from responders at BR. R_PD: the plasma collected from responders at PD. [#]1. Platelet activation; 2. Cell activation; 3. Blood coagulation; 4. Hemostasis; 5. Coagulation; 6. Cellular response to granulocyte colony-stimulating; 7. Negative regulation of blood coagulation; 8. Regulation of blood coagulation; 9. Blood coagulation, common pathway; 10. Response to granulocyte colony-stimulating factor; 11. Platele alpha granule; 12. Blood microparticle; 13. Mucus layer; 14. Cell cortex; 15. Cytoplasmic region; 16. Fibrinogen complex; 17. Membrane-bounded vesicle; 18. Extracellular space; 19. Vesicle; 20. Secretory granule.

Figure 4

Analysis of the differential protein levels between baseline and best response in anlotinib non-responders.
(a) Heat map representation of protein differentially levels between NR_BL and NR_PD[*]. Each group
contained 2 duplicate samples. The one sample represented the mean data of patients No. 1-7, and the
other one represented the mean data of patients No. 8-14. (b) Biological process and cell component
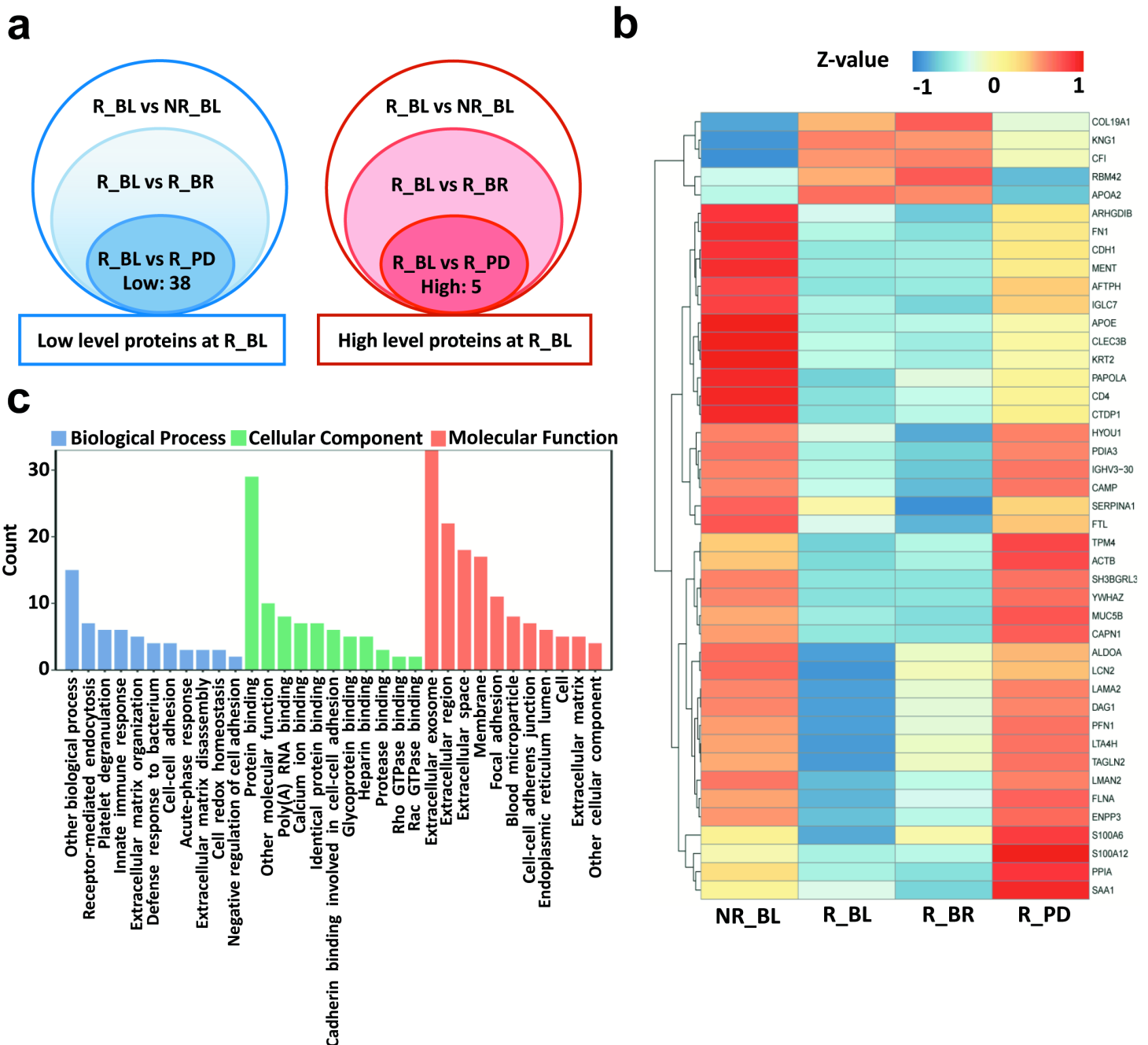analysis for those differential proteins[#]. (c) Biological process analysis for those up-regulated and down-

regulated proteins respectively. *NR_BL: the plasma collected from non-responders at BL. NR_PD: the plasma collected from non-responders at PD. #1. Inflammatory response; 2. Cell migration; 3. Localization of cell; 4. Cell motility; 5. Keratinocyte migration; 6. Leukocyte migration; 7. Locomotion; 8. Cytokine secretion; 9. Acute inflammatory response; 10. Movement of cell; 11. Extracellular region; 12. Extracellular region part; 13. Cytoplasmic membrane-bounded vesicle lumen; 14. Vesicle lumen; 15. Extracellular space; 16. Extracellular exosome; 17. Extracellular vesicle; 18. Extracellular organelle; 19. Vesicle; 20. Blood microparticle.
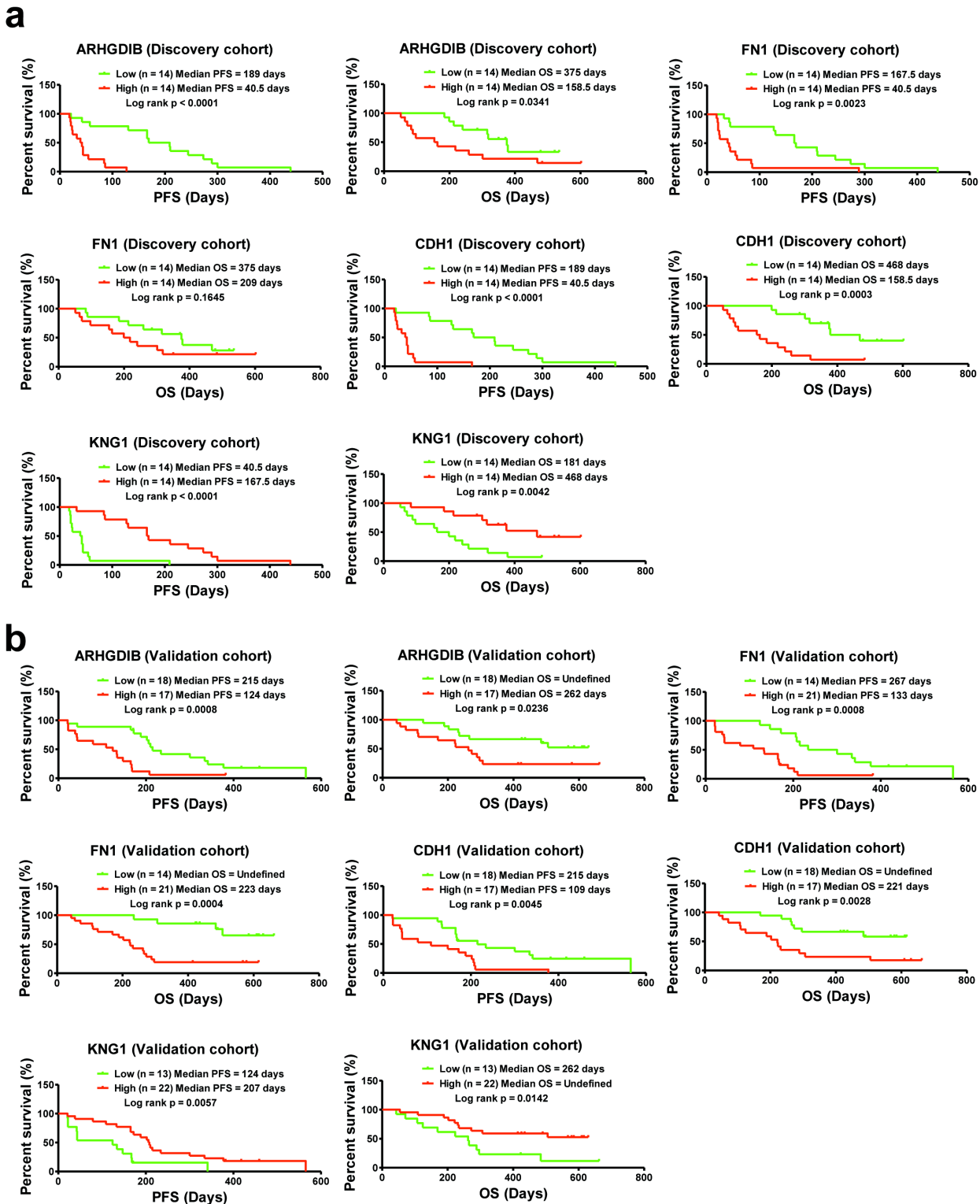
Figure 5

Analysis of the differential protein levels between responders and non-responders at baseline. (a) Scatter plot analysis of the differential proteins (R_BL / NR_BL)[*]. (b) Heat map representation of protein differentially levels between responders and non-responders at BL. Each group contained 2 duplicate samples. The one sample represented the mean data of patients No. 1-7, and the other one represented the mean data of patients No. 8-14. (c) Biological process and cell component analysis for those

differential proteins[#]. (d) Biological process analysis for those up-regulated and down-regulated proteins respectively. [*]R_BL: the plasma collected from responders at BL. NR_BL: the plasma collected from non-responders at BL. [#]1. Peptide cross-linking; 2. Keratinocyte activation; 3. Skin epidermis development; 4. Cornification; 5. Regulation of peptidase activity; 6. Positive regulation of substrate-dependent cell; 7. Regulation of substrate-dependent cell migration; 8. Interaction with other organism; 9. Negative regulation of transforming growth; 10. Calcium-independent cell-matrix adhesion; 11. Extracellular space; 12. Extracellular region part; 13. Extracellular region; 14. Cornified envelope; 15. Extracellular membrane-bounded organelle; 16. Insulin-like growth factor binary complex; 17. Extracellular exosome; 18. Extracellular vesicle; 19. Extracellular organelle; 20. Keratin filament.

Figure 6

Integrative analysis of plasma protein levels between responders and non-responders at different time points. (a) The diagrammatic figure of integrative analysis for screening the candidate differential proteins[*]. (b) Heat map representation of protein differentially levels between responders and non-responders at different time points. Each group contained 2 duplicate samples. The one sample represented the mean data of patients No. 1-7, and the other one represented the mean data of patients No. 8-14. (c) Analysis biological process, cell component and molecular function for those differential proteins. [*] R_BL: the plasma collected from responders at BL. R_BR: the plasma collected from responders at BR. R_PD: the plasma collected from responders at PD. NR_BL: the plasma collected from non-responders at BL.

Figure 7

The differential proteins at baseline potentially be used as biomarker for anlotinib response. (a) Kaplan-Meier plots of PFS and OS in the advanced refractory NSCLC patients treated with anlotinib from discovery cohort based on plasma ARHGDIB, FN1, CDH1, and KNG1 levels respectively. *n* = 28, Cutoff-High: 14 patients, Cutoff-Low: 14 patients. (b) Kaplan-Meier plots of PFS and OS via stratifying the plasma ARHGDIB, FN1, CDH1, and KNG1 levels respectively, upon the advanced refractory NSCLC

patients treated with anlotinib in validation cohort. *n* = 35, Cutoff-High: 17 patients, Cutoff-Low: 18 patients.
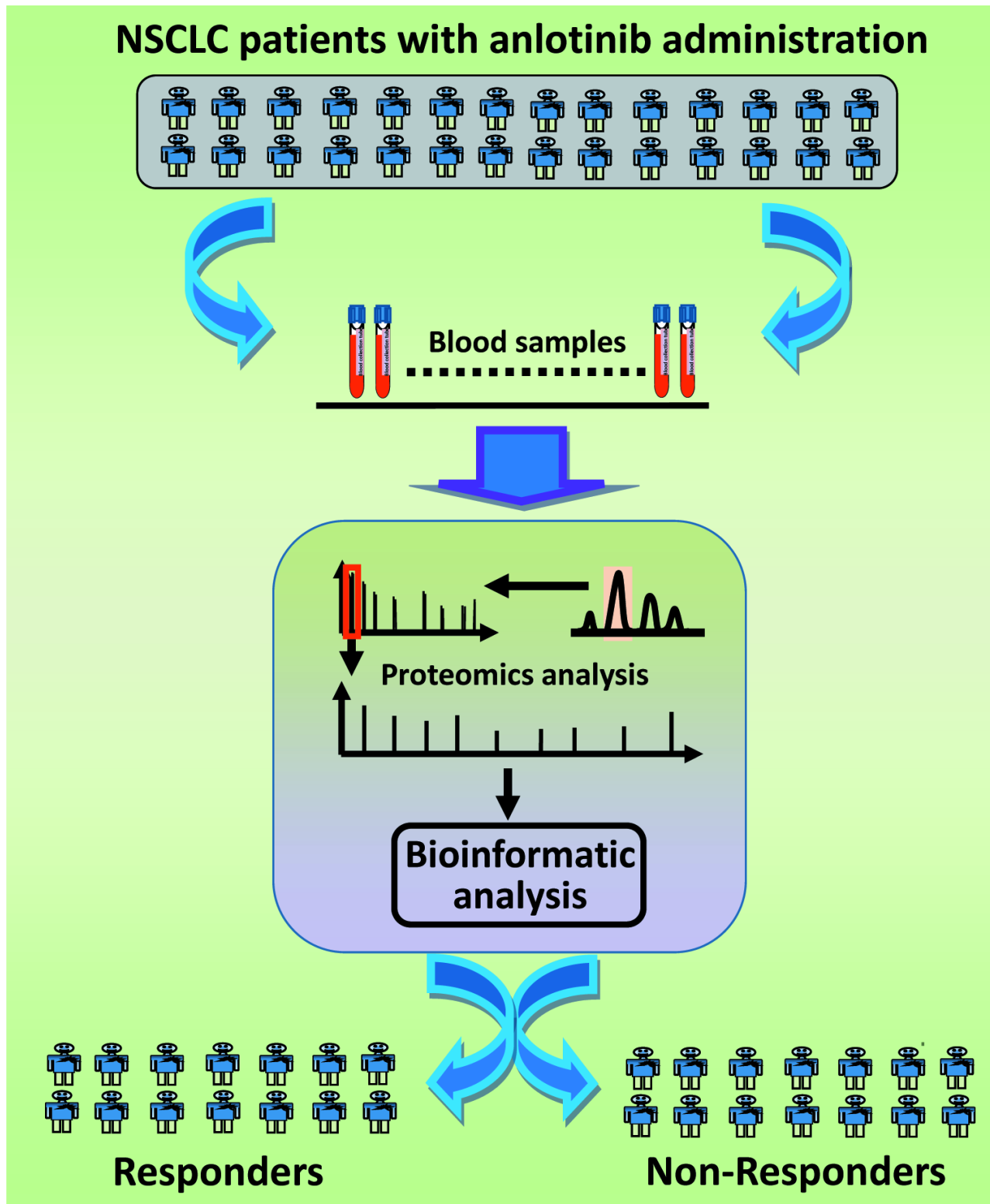

Figure 8

The flowchart of screening anlotinib responders and anlotinib non-responders via proteomics analysis.

Supplementary Files

This is a list of supplementary files associated with this preprint. Click to download.

- Supplementarydata.pdf